Journal of Alloys and Compounds 509 (2011) 3038–3041

Contents lists available at ScienceDirect

Journal of Alloys and Compounds

journal homepage: www.elsevier.com/locate/jallcom

NiCuZn ferrite flakes prepared using a sol–gel bubble method and its magnetic properties

Z.H. Yang*, Z.W. Li, L. Liu, L.B. Kong

Temasek Laboratories, National University of Singapore, 5A Engineering Drive 1, Singapore 117411, Singapore

ARTICLE INFO

Article history:
Received 23 July 2010
Received in revised form
30 November 2010
Accepted 30 November 2010
Available online 8 December 2010

Keywords:
NiCuZn ferrites
Flakes
Sol–gel process
Magnetic properties

ABSTRACT

$Ni_{0.23}Cu_{0.11}Zn_{0.66}Fe_2O_4$ ferrite flakes, with thickness of about 8 μm and average diameter of 20–35 μm, were prepared using a sol–gel bubble method. Morphology, phase evolution, static and dynamic magnetic properties of the flakes and their composites were studied. Magnetic measurements showed that easy magnetization direction of the flaky filler composite was parallel to its sample plane. Composites made of silicone resins and flakes had higher complex permeability, which can be attributed to the reduction in demagnetization factor due to their flaky shapes. This sol–gel bubble method should be also applicable to fabricating flakes of other multi-component oxides.

1. Introduction

Ferrites are commercially important functional materials because of their excellent magnetic and electrical properties [1,2]. Among various ferrite materials, the NiZn ferrites are considered as the most versatile soft magnetic materials due to their high resistivity, high permeability and low eddy current loss for high frequency applications [3–6]. Recently, various studies showed that the addition of copper in NiZn ferrites could tune the magnetic properties [7,8]. As a result, NiCuZn ferrites have been widely used to fabricate multilayer chip inductors (MLCI) and electromagnetic interference (EMI) filters [9,10]. Additionally, NiCuZn ferrites are also promising candidates for microwave attenuating composite materials [11].

Various methods, such as conventional ceramic process [10], hydrothermal [12], sol–gel [13,14], and co-precipitation [15–17], have been used to synthesize ferrite powders. Generally, ferrites prepared using these methods are particles of irregular shapes. However, it has been shown that, ferrites with flaky shapes could have enhanced permeability due to the reduced demagnetization factor caused by their anisotropic structural characteristics [18]. Moreover, polymer matrix composite materials with flaky fillers would have advanced mechanical properties in specific fields of applications [19]. To the best of our knowledge, there has been no report on synthesis of NiCuZn ferrite flakes. So in this work, we demonstrate a one-step and cost-effective solution phase chemical method to prepare NiCuZn ferrite flakes. Composites made of the flakes and silicone resins were characterized in terms of microwave performances.

2. Experimental procedures

2.1. Preparation of $Ni_{0.23}Cu_{0.11}Zn_{0.66}Fe_2O_4$ flakes and composites

Analytical grade $Ni(NO_3)_2{\cdot}6H_2O$, $Cu(NO_3)_2{\cdot}6H_2O$, $Zn(NO_3)_2{\cdot}6H_2O$, $Fe(NO_3)_3{\cdot}9H_2O$ and citric acid ($C_6H_8O_7{\cdot}H_2O$), supplied by Alfa Aesar (USA), were used as starting materials. The metal salts and citric acid were separately dissolved in deionized water, with concentrations of 0.1 M and 0.2 M, respectively. According to the molar ratio of citrate to metal ions of CA:Fe^{3+}:(Ni^{2+} + Cu^{2+} + Zn^{2+}) = 4.5:2:1, the metal salt solution was gradually added into the citric acid solution with continuous stirring using a magnetic stirrer. pH value of the solution was maintained to be 5 by the addition of ammonia solution. The final solution was stirred for 20 h at room temperature. The obtained solution was then evaporated on a hot plate at 60–70 °C to remove surplus water until a viscous sol was obtained. Some viscous sol was dripped into a culture dish using a burette as shown in Fig. 1(a). The culture dish was then placed into a vacuum oven at 60 °C. Under the vacuum environment, the viscous sol drops expanded to form gel bubbles, as shown in Fig. 1(b). The gel bubbles were collected and annealed in a quartz crucible at 1000 °C for 2 h in ambient atmosphere. The gained NiCuZn ferrite bubbles were crushed into particles using an agate pestle and mortar. For comparison, usual irregular particles were also prepared. Powders prepared by auto-combustion technique using the same NiCuZn ferrite sol were subjected to press compacting to a platelet shape with a diameter of 15 mm and thickness of approximately 5 mm and annealed under same condition as the gel bubbles. The platelet was also hand-ground into particles using an agate pestle and mortar.

Flaky filler and irregular filler composites were prepared by mixing silicone resin with 20 vol.% $Ni_{0.23}Cu_{0.11}Zn_{0.66}Fe_2O_4$ flakes and irregular particles, respectively. Aligned flaky filler composites were prepared by applying a magnetic field of about 0.6 T parallel to plane of the composites using permanent magnets before the silicon resin solidified. This process ensured that the flakes were aligned to each

* Corresponding author. Tel.: +65 65165368; fax: +65 68726840.
E-mail address: tslyzh@nus.edu.sg (Z.H. Yang).

0925-8388/$ – see front matter © 2010 Elsevier B.V. All rights reserved.
doi:10.1016/j.jallcom.2010.11.195

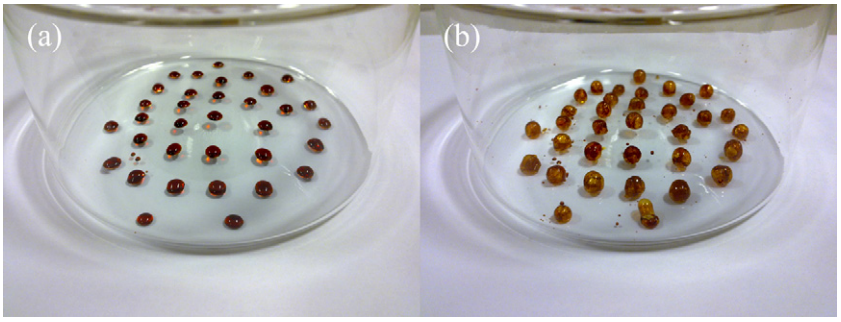

Fig. 1. Photographs of the viscous sol drops before (a) and after (b) being bubbled.

other and the flake plane was also parallel to the sample plane. For measurement of static magnetic properties, samples were made into a small cylinder, with a diameter of 4.0 mm and thickness of 2.0 mm. For measurement of microwave properties, samples were made into toroidal shape, with an outer diameter of 7.0 mm, inner diameter of 3.0 mm, and thickness of 2.0 mm.

2.2. Characterization

Morphologies of $Ni_{0.23}Cu_{0.11}Zn_{0.66}Fe_2O_4$ flakes and irregular particles were characterized by means of scanning electron microscopy (SEM, JEOL JSM 6500). Effects of processing methodologies on alignment of the flake-based fillers in the composites were also studied using SEM. X-ray diffractions (XRD) pattern of the samples were measured using a Riguka D/Max2200PC diffractometer with Cu-Kα radiation. Magnetization curves M(H) and magnetic hysteresis loops were measured to determine the easy-magnetization directions, using a vibrating sample magnetometer (VSM, ADE magnetics EV-7, USA) at room temperature. The composites were measured both parallel and perpendicular to the sample plane of the cylindrical-shaped composites.

Complex permeability and permittivity of the composites were measured over 0.1–16 GHz using HP 8722D network analyzer (VNA) with through-reflection-line calibration. The measurement fixture is 29.96 mm coaxial line. Also, complex permeability at lower frequency (0.001–1 GHz) was measured using

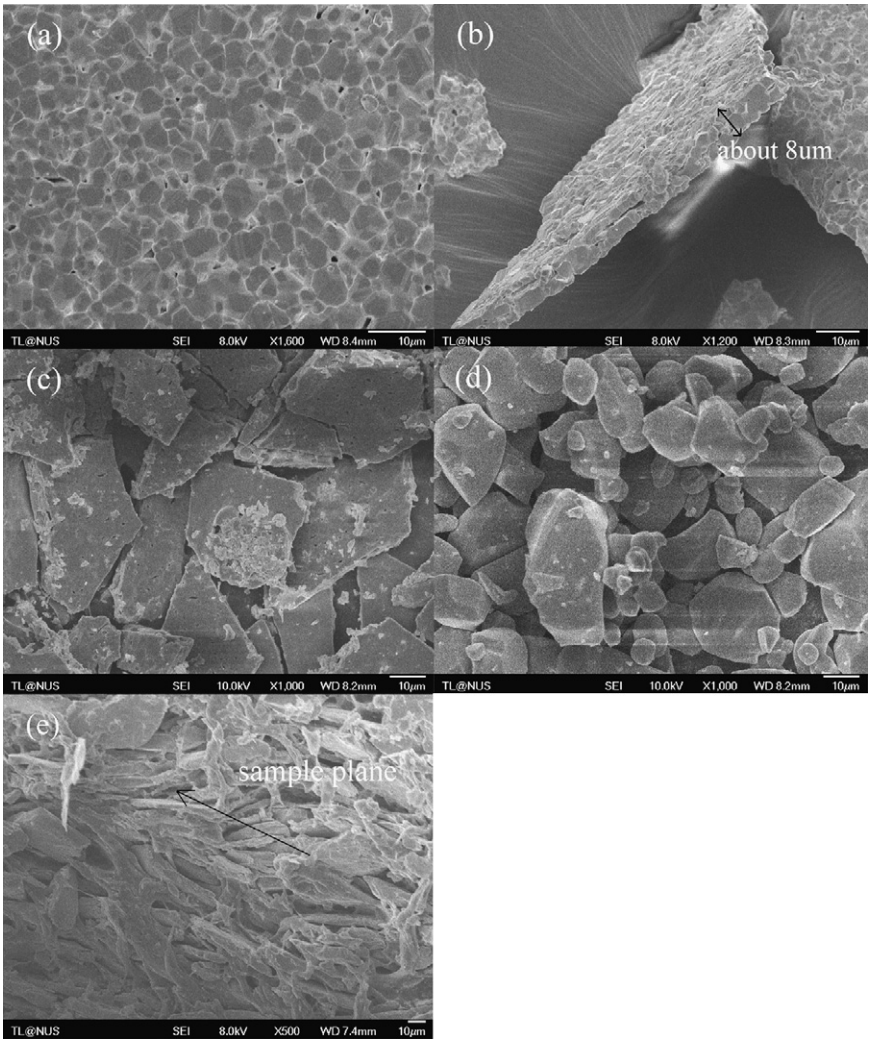

Fig. 2. SEM images of the $Ni_{0.23}Cu_{0.11}Zn_{0.66}Fe_2O_4$ powders and composites: (a) grain morphology of the flakes, (b) cross-section of a flake, (c) low magnification image of flakes, (d) irregular particles, and (e) cross-section of the flaky filler composite.

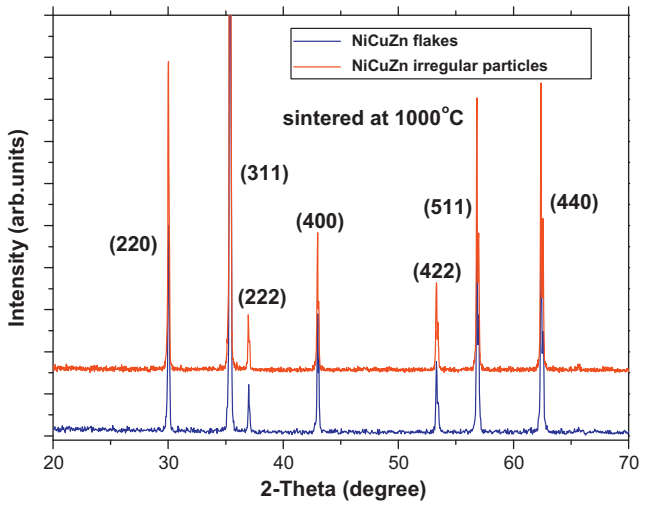

Fig. 3. XRD patterns of the $Ni_{0.23}Cu_{0.11}Zn_{0.66}Fe_2O_4$ flakes and irregular particles.

Agilent E4991A RF impedance/materials analyzer with open-short-load calibration.

3. Results and discussion

3.1. Structure and morphology

Fig. 2 shows SEM images of the $Ni_{0.23}Cu_{0.11}Zn_{0.66}Fe_2O_4$ irregular particles, flakes and the cross-section of flaky filler composite. As shown in Fig. 2(a), the flakes consist of small grains with 3–5 μm. Fig. 2(b) and (c) indicates that the flakes have a thickness of about 8 μm and an average diameter of 20–35 μm. And the irregular particles have an average size of 15–40 μm, as shown in Fig. 2(d). Fig. 2(e) indicates that most flakes in the silicone resin are approximately oriented parallel to the sample plane. Fig. 3 shows XRD patterns of the $Ni_{0.23}Cu_{0.11}Zn_{0.66}Fe_2O_4$ flakes and irregular particles. All the samples have a single phase with cubic spinel structure. No additional lines corresponding to any other phase are detected.

3.2. Magnetic properties

Fig. 4 shows magnetization curves $M(H)$ and magnetic hysteresis loops of the flaky filler and irregular filler composites. Table 1 lists the static magnetic properties of the flaky filler and irregular filler composites. The shapes of magnetic hysteresis loops of the flaky filler composite are found to be dependent on orientation of the sample plane to applied magnetic field (H). The significant difference in shape of the loops is attributed to the different demagnetizing factors of flakes in the composite, as the sample plane is parallel and perpendicular to the direction of applied magnetic field. Saturation magnetization (M_s) of the flaky filler composite is about 33.6 emu/g, which is slightly smaller than that of the irregular filler composite (34.3 emu/g). For the flaky filler composite, in-plane and out-of-plane coercivities (H_c) are 12.9 and 16.7 Oe, respectively, both of which are slightly higher than that of the irregular filler composite (10.7 Oe).

Table 1
Magnetic properties of the composites with $Ni_{0.23}Cu_{0.11}Zn_{0.66}Fe_2O_4$ ferrite flaky filler and irregular filler.

Sample	H_c (Oe)	M_s (emu/g)
Aligned flaky filler composite (// H)	12.9	33.7
Aligned flaky filler composite (⊥ H)	16.7	33.6
Irregular filler composite	10.7	34.3

3.3. Microwave magnetic and dielectric properties of the composites

Complex permeability ($\mu = \mu' - j\mu''$) curves of the composite samples with flaky filler and with irregular filler are shown in Fig. 5. μ' values of the two samples at 1 MHz are 8.1 and 4.2, respectively. Maximum imaginary permeability μ'', corresponding to the resonance frequency f_r, of the flaky filler composite is 2.48, which is higher than that of the irregular filler composite by 135%. The flaky filler composite has a resonance frequency of 0.06 GHz, while the resonance frequency of the irregular filler composite is 0.23 GHz.

As shown above, particle sizes of the flaky and irregular fillers are in the same range and they also have close values of M_s and H_c. Therefore, the difference in initial permeability and resonance frequency (f_r) between the two composites is mainly attributed to the different demagnetizing factors (N_d). It is known that effective permeability (μ_{eff}) of a composite is closely related to demagnetizing factor (N_d) based on the mixing laws [20–22]:

$$\mu_{eff} = 1 + \frac{(\mu_b - 1)p}{(\mu_b - 1)(1-p)N_d + 1} \quad (1)$$

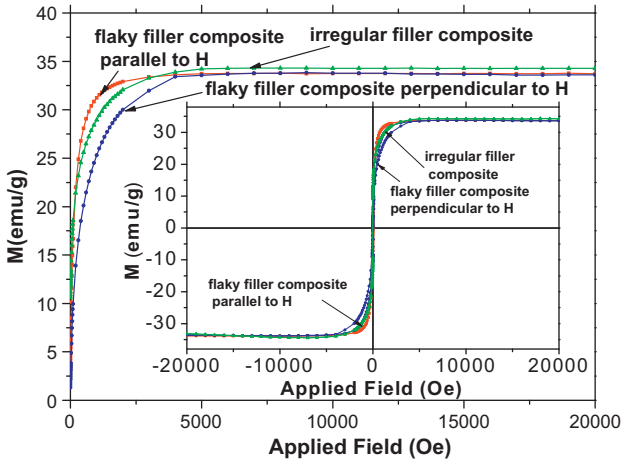

Fig. 4. Magnetization curve $M(H)$ and magnetic hysteresis loops both parallel and perpendicular to the applied magnetic field for aligned flaky filler and irregular filler composites.

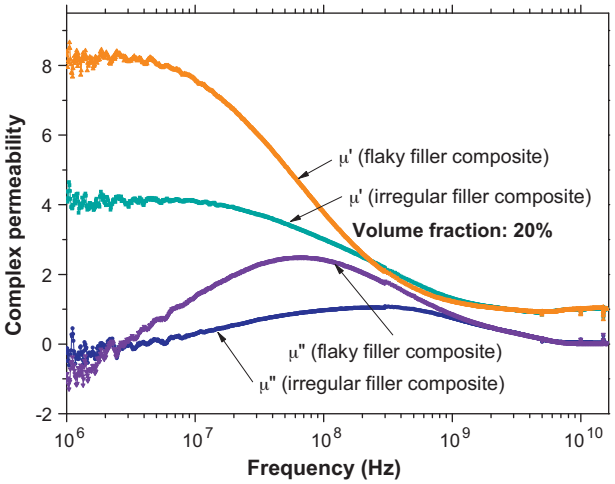

Fig. 5. Complex permeability of the flaky filler and irregular filler composites.

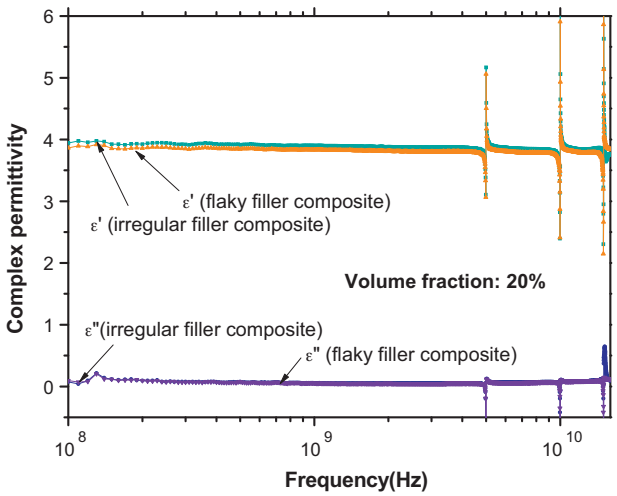

Fig. 6. Complex permittivity of the flaky filler and irregular filler composites.

where μ_b is the initial permeability of corresponding bulk material, p is the volume concentration of ferrite in the composite and N_d is demagnetizing factor. It has been reported that flakes have much smaller demagnetizing factor than irregular particles [18,23]. Therefore, smaller demagnetizing factor (N_d) leads to larger effective permeability for same μ_b. In addition, without an applied magnetic field, resonance frequency is mainly determined by anisotropy field and demagnetizing field. The magnitude of demagnetizing fields is proportional to N_d. Consequently, due to its smaller N_d, the flaky filler composite has lower resonance frequency than the irregular filler composite.

Fig. 6 shows complex permittivity of the composites with flaky and with irregular fillers. Both real part (ε') and imaginary part (ε'') are almost constant over 0.1–16 GHz. The real part ε' of the flaky filler composite is about 3.86 while that of irregular filler composite is about 3.94. Since $Ni_{0.23}Cu_{0.11}Zn_{0.66}Fe_2O_4$ ferrite is an insulating material, ε' and ε'' values of its composites are mainly determined by its bulk permittivity (ε_b) and its volume fraction in the silicone matrix. In this case, shapes of the particles have no effect on the permittivity values of the composites.

4. Conclusions

$Ni_{0.23}Cu_{0.11}Zn_{0.66}Fe_2O_4$ ferrite flakes were prepared via a sol–gel bubble method. The flakes had grain sizes of 3–5 μm and a thickness of about 8 μm. The aligned flaky filler composite had hysteresis loops dependent on their orientations to the applied magnetic field (H). Saturation magnetization (M_s) of the flaky filler composite was 33.6 emu/g, while their in-plane and out-of-plane coercivities (H_c) were 12.9 and 16.7 Oe, respectively. The composite with flaky filler had greatly increased complex permeability, as compared to the composite with usual irregular filler. It is expected that the method developed in the present work is also applicable to the preparation of other oxide flakes.

Acknowledgements

This work was supported by the Defence Research and Technology Office (DRTech), Ministry of Defence, Singapore.

References

[1] L.B. Kong, Z.W. Li, G.Q. Lin, Y.B. Gan, J. Am. Ceram. Soc. 90 (2007) 2104.
[2] M. Sugimoto, J. Am. Ceram. Soc. 82 (1999) 269.
[3] P. Priyadharsini, A. Pradeep, P. Sambasiva Rao, G. Chandrasekaran, Mater. Chem. Phys. 116 (2009) 207.
[4] D.W. Guo, Z.M. Zhang, M. Lin, X.L. Fan, G.Z. Chai, J. Phys. D 42 (2009) 125006.
[5] Q.L. Li, Y.F. Wang, C.B. Chang, J. Alloys Compd. 505 (2010) 523.
[6] A.C.F.M. Costa, A.P. Diniza, V.J. Silva, et al., J. Alloys Compd. 483 (2009) 563.
[7] D.L. Zhao, Q. Lv, Z.M. Shen, J. Alloys Compd. 480 (2009) 634.
[8] M.A. Gabal, Y.M. Al Angari, S.S. Al-Juaid, J. Alloys Compd. 492 (2010) 411.
[9] M. Kaiser, J. Alloys Compd. 468 (2009) 15.
[10] H. Su, H.W. Zhang, X.L. Tang, Z.Y. Zhong, Y.L. Jing, Mater. Sci. Eng. B 162 (2009) 22.
[11] H. Su, H.W. Zhang, X.L. Tang, Y.L. Liu, J. Mater. Sci. 42 (2007) 2849.
[12] Y.P. Fu, J. Am. Ceram. Soc. 89 (2006) 3547.
[13] P.A. Jadhav, R.S. Devan, Y.D. Kolekar, B.K. Chougule, J. Phys. Chem. Solids 70 (2009) 396.
[14] S.F. Yan, J.B. Yin, E.L. Zhou, J. Alloys Compd. 450 (2008) 417.
[15] J.S. Kim, C.W. Ham, Mater. Res. Bull. 44 (2009) 633.
[16] H.B. Wang, J.H. Liu, W.F. Li, et al., J. Alloys Compd. 461 (2008) 373.
[17] J.C. Aphesteguy, S.E. Jacobo, N.N. Schegoleva, G.V. Kurlyandskaya, J. Alloys Compd. 495 (2010) 509.
[18] Z.W. Li, Z.H. Yang, L.B. Kong, Appl. Phys. Lett. 96 (2010) 092507.
[19] P. Podsiadlo, A.K. Kaushik, E.M. Arruda, et al., Science 318 (2007) 80.
[20] J.C. Maxwell Garnett, Phil. Trans. R. Soc. London Ser. A 203 (1904) 385.
[21] O. Acher, A.L. Adenot, Phys. Rev. B 62 (2000) 11324.
[22] R.K. Walser, W. Win, P.M. Valanju, IEEE Trans. Magn. 34 (1998) 1390.
[23] G.Q. Lin, Z.W. Li, L.F. Chen, Y.P. Wu, C.K. Ong, J. Magn. Magn. Mater. 305 (2006) 291.